

Through process effects on final Al-sheet flatness

S. Neumann, K.F. Karhausen

Hydro Aluminium Rolled Products GmbH, R&D, Georg-von-Boeselagerstr.21, 53117 Bonn, Germany

Keywords: Through process modelling, rolling, winding, creep, flatness

Abstract

To achieve the desired flatness of rolled aluminium products in ever decreasing tolerances becomes more and more a key challenge. The typical process chain of strip material consists of hot rolling, cold rolling, annealing as well as coil winding and unwinding at various stages. Primarily the product flatness is dominated by the profile and internal stress generation during the rolling steps. However, in the coil some aluminium alloys show a strong tendency to reduce internal stresses by creep and relaxation. This transformation of elastic into plastic strains frequently leads to considerable changes of shape and flatness of the product over the different steps of the process chain.

This paper introduces a model based through process analysis with emphasis to the evolution of strip flatness via the most decisive production stages. A case study from aluminium strip production is used to illustrate the impact of different process parameters.

Introduction

The rolling production process of Al-sheet involves a large number of processing steps like hot and cold rolling, annealing, slitting, surface treatments and further downstream processing. In-between many of these stages, the material is coiled and de-coiled again. Besides the impact of the original rolling passes on shape and flatness, the coiling has a large impact, since considerable stresses are induced throughout the coil build up. Due to the nature of this particular processing chain in conjunction with the specific material behavior of aluminium there is a strong interaction between the sequential steps with cumulative effects which may reveal at the final product.

A typical example in this context is the final flatness quality when a plate is cut out of a coil. Generally speaking, the flatness of a strip has to be regarded as evolving with respect to the particular stage of the process chain. The condition of the strip is strongly dependent on:

- material properties of the product, e.g. temper and alloy
- thickness profile as produced and evolving throughout the rolling
- winding conditions at the various steps
- set-up of the cutting tools
- temperature history of the coil

In industrial practice a given target shape is usually attained during rolling due to the available modern shape control systems. But practice shows that considerable flatness or shape deviations may still occur in the final processing stages at the slitter or in finishing lines. Accordingly a precise knowledge of the process mechanisms and their impact on the final product condition is required to detect and to avoid the nucleus of such problems. Due to the large number of process steps with an even larger number of processing parameters, it is time consuming and costly to optimize the process chain by trial and error. The development of simulation tools is required to model the flatness and shape effects of the consecutive process stages

- hot rolling

- cold rolling
- winding and unwinding
- coil storage
- coil annealing

The models need to be coupled to enable the tracing of profile, shape and flatness through a particular production chain, i.e. a Through Process Model (TPM) for matching the complete process sequence is demanded.

Through process analysis

The objective of this work is to present results of a through process analysis with emphasis on final flatness quality. In particular it is the objective to study the impact of rolling parameters to the flatness of a plate that has been cut of the final coil.

To this end our recent ambitions have been concentrated on filling the gap between the various in-house developments as well as commercial tools towards a TPM for flat rolled aluminium products. The analysis is based on a stepwise simulation of:

1. Hot and cold rolling to calculate the thickness profile and residual stresses of the strip
2. Coiling at the final cold rolling step to predict the wound in stresses
3. The evolution of creep strains in the coil when being stored
4. The flatness in the final strip when the residual stresses are released on unwinding and cutting

Note that the first simulation steps, i.e. rolling and winding simulations, are based on software tools that have been developed in-house whereas the two final steps involve the application of the commercial FE-package ABAQUS®.

Hot rolling

The hot rolling operation starts with an ingot thickness of typically 350-600 mm, which is rolled down to a hot strip of a thickness in-between 3-6 mm in several reversing passes. Depending on the mill set-up, the final two to four passes can also be performed in a continuous tandem line. While the ingot is usually cast into a rectangular cross profile, the strip gradually assumes a "cigar" like profile. To some extent this form is desired, since it is beneficial for cold rolling and following processing steps. However it needs to be controlled within a desired window. The profile essentially results of the bending of the rolls under load, work roll flattening, thermal expansion, tensile stresses, material properties, etc. Conventionally it can be controlled by choosing an appropriate work roll crown, by active work roll bending and local cooling. Furthermore, there are a number of more advanced actuators available on modern mills.

A coupled model for predicting profile and shape has been developed in-house and is used for a sample analysis. The principles are described in [1]. Most notable is the necessity of coupling the longitudinal stresses in the strip, generated by profile changes, with the roll gap model [2], which takes place iteratively in this model without introducing further empirical factors.

Furthermore a thermal roll model is implemented to trace the temperature development over larger pass schedules.

In this case a simple reversing mill is assumed for a pass schedule of alloy AA1200 of 1400 mm width. A work roll crown of $0.4 \mu\text{m}$ has been set and no active work roll bending was applied. Since at high enough temperatures, the material usually does not develop residual stresses, only the profile of the final strip, in this case of 5 mm centre thickness, is the relevant characteristic for the following cold rolling.

In this case the development of temperature at the mill has a great impact. For the model example, the mill was started without any initial thermal profile and simulation results are presented in fig. 1 for the first strip in this condition as well as for the following 5th, 10th and 20th strip, where the thermal profile of the rolls has developed.

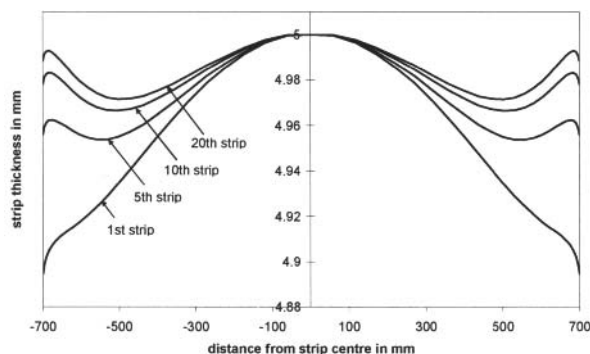


Figure 1: Thickness profile development during hot rolling

If no further measures are taken with eventually available mill actuators, it can be seen that the thermal profile on the work rolls strongly influences the strip profile. While the first strip has a desired cigar shape, the magnitude of 2% is very high. The profile heights is greatly diminished towards the 20th strip, where it only amounts to 0.2%, but now undesired up-coming edges are observed. The impact of these two extreme cases is analyzed in the following.

Cold rolling

In the present case study, the strip is cold rolled to 0.28 mm. Essentially only the first pass can introduce further small profile changes. With decreasing strip thickness, a profile deformation will lead to shape problems, essentially making a stable cold rolling impossible. Thus, in the simulation the cold rolling conditions (work roll crown, bending) were set in order not to introduce great profile changes, as done in rolling practice.

The profile change of the first cold pass from 5 to 2.3 mm is presented in fig. 2. Here the true calculated profile is compared to the proportional profile which would result if the initial profile remained unchanged. The total profile deviation is already very small in this pass and will be even smaller in subsequent passes. Consequently, it is not useful to simulate all further cold rolling passes which do not affect the profile anymore.

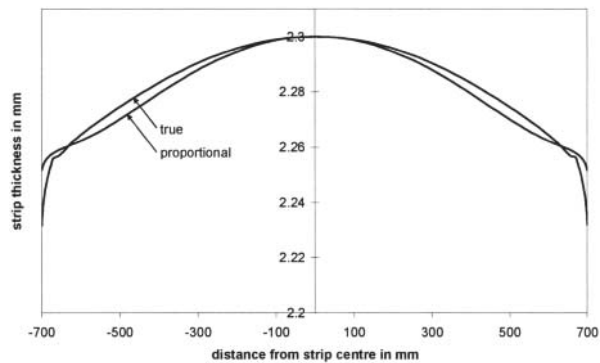


Figure 2: Thickness profile of hot strip 1 after following cold pass

Winding

The winding in-between passes has no impact on final strip flatness, since the complete plastification in the subsequent pass will remove all pre-existing residual stresses. However it can influence the performance of this pass. But the final coiling operation is decisive for the strip quality. Throughout the coil built up large stresses can be generated. This stress state has to be regarded since the coil stability as well as the strip quality is affected. Simulation tools derived to model the winding process and to calculate the wound in stresses due to the different winding parameters proved to be an effective assistant for process optimization, c.f. [3]. In this study a winding software is applied that was initially derived by [4] and was further enhanced as outlined in [5]. The tool treats the winding process basically under the following assumptions:

- The coil is a coherent body, i.e. no contact conditions between single laps
- The coil material is non-linear elastic and transversal orthotropic
- The coil is an assembly of stacks of layers, each with “equivalent material behavior” as the (macroscopic) coil
- 2D axisymmetric geometrical and loading conditions

It accounts for the most important process parameters of centre drive winding, namely the incoming residual stresses of the strip, the strip thickness profile, the spool material and geometry and the winding tension profile.

Concerning the two case studies under consideration, the final flatness of the strip is mostly affected by the conditions of the coiling at the last cold rolling step. It is assumed that the thickness profile remains unchanged after cold rolling to 2.3 mm. The thickness profiles can then be downscaled to the final nominal thickness of 0.28 mm to perform the winding simulation after the final cold rolling. The following parameters have been assumed for this winding step:

- Constant winding tension of 30 MPa
- Steel spool with 480 mm inner diameter and thickness of 35 mm
- Coil outer diameter of 1740 mm
- Nominal strip thickness of 0.28 mm with profiles according to fig. 1, 1st and 20th strip
- Constant strip and spool temperature of 140°C

With a view on flatness effects it is the hoop stress which is most relevant. Fig. 3 illustrates the wound in hoop stress in a cross

section of coil 1. The stress distribution is typical for a wound strip with a cigar shaped thickness profile which cumulates to a barrel. According to the larger diameter at the centre of coil 1 large tensile stresses at the outer wraps are formed, indicated by the bright domain. This stress component will be discussed in more detail in figs. 4 and 5, which present cross sectional cuts of the hoop stress for both coils according to the positions shown in fig 2.

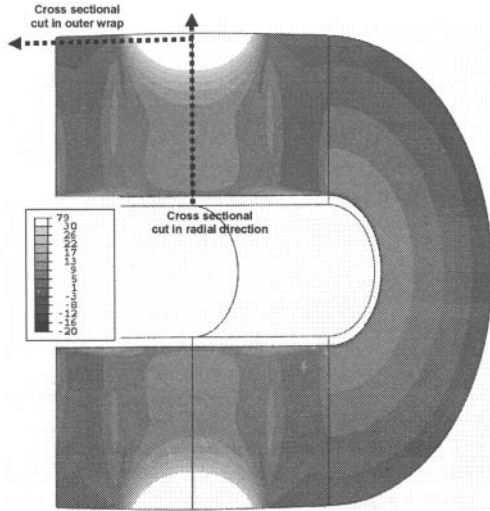


Figure 3: Hoop stress for a cross section of coil 1.

The difference in hoop stress on a radial cut in both coils (fig. 4) is quite drastic. Due to the large crown of the thickness profile of coil 1 the barrel shape is more pronounced as compared to coil 2. Accordingly, large tensions up to a maximum of 80 MPa act on the strip centre towards the outer wraps. The thickness profile of coil 2 has a comparatively large bearing fraction. In general this is regarded to be positive since the tensions in the outer wraps at the coil centre are minimized. The present results show, that the large bearing fraction drops the hoop stress by ~35% to a value of 53 MPa. In both cases the results reveal a compressive hoop stress at the vicinity of the spool. This indicates a considerable necking of the spool and, accordingly, the inner wraps are compressed.

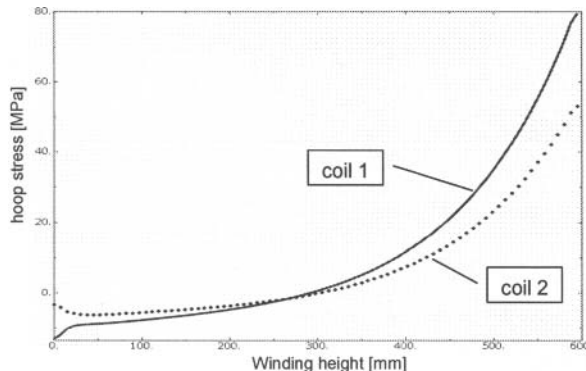


Figure 4: Hoop stress of cross sectional cuts in radial direction after winding (see fig. 3)

Fig. 5 illustrates the hoop stress distribution of both coils in strip width direction at the outer wrap. The upcoming edges of coil 2

prove to be detrimental and outweigh the benefit of the large bearing fraction. Due to the upcoming edges the outer wraps of coil 2 develop an additional tension peak with a maximum value of 43 MPa at the vicinity of the edges.

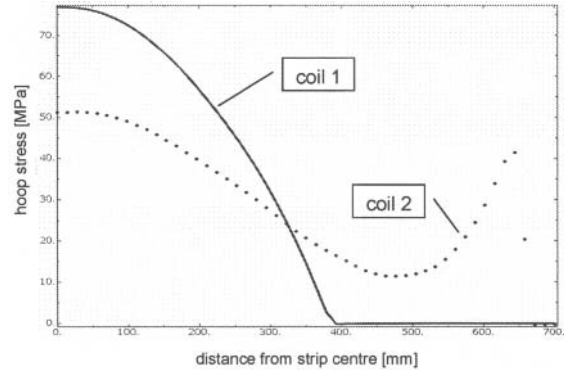


Figure 5: Hoop stress for cross sectional cuts in the outer wrap after winding (see fig. 3)

Storage

The winding simulation of the previous section assumes pure elastic material behavior and neglects thermal aspects. The calculations reveal that the winding step produces considerable stresses inside the coils with significant differences between both coils. Certain aluminium alloys show a tendency to level internal stresses by creep and relaxation already at room temperature and at comparative low stress levels. The corresponding mechanisms are strongly temperature dependent and can cause severe changes of the flatness inside the coils during storage. To account for the effects related to creep and relaxation a consecutive FE-analysis is applied using the commercial the FE software ABAQUS. Based on the results of the winding simulation a 2D-axisymmetric FE-model is prepared for the coils. As in the previous section the coil is modeled as a coherent body whereas contact between spool and coil is involved in the following. A phenomenological approach for modeling creep is applied where the resulting strain rate $\dot{\epsilon}_{cr}$ follows a power law:

$$\dot{\epsilon}_{cr} = \left(A \sigma_v^n \left[(m+1) \epsilon_{cr} \right]^m \right)^{1/m} \quad (1)$$

where σ_v denotes the von Mises stress and ϵ_{cr} the equivalent creep strain, c.f. [6]. Constants A , n and m are experimentally predicted for the alloy by isothermal tests. Fig. 6 shows the results of creep tests on the present alloy conducted with applied tensions of 10, 20, and 60 MPa, being a representative range for the wound in stresses.

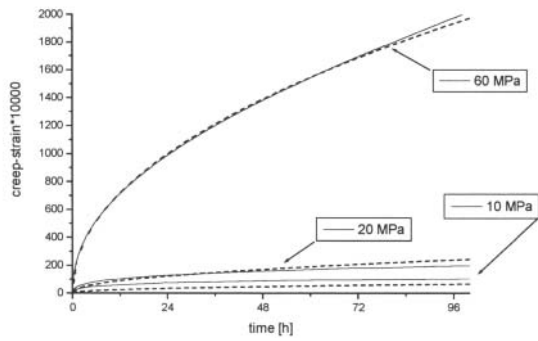


Figure 6: Stress relaxation measurements at room temperature

The stress relaxation simulations were conducted under the conditions, that the coils were stored for 5 days. During storage the coils cool down from an initial temperature of 140°C of the last rolling pass to room temperature. The initial stress distribution is transferred from the previous simulations.

Fig. 7 shows the hoop stress of the radial centre cut of both coils after storage. The stress distributions of both coils are very similar and the maximum difference in hoop stress has dropped to 5 MPa. The cooling effect of the coils becomes visible at the vicinity of the spool. Due to the different thermal expansion coefficients of spool and coil, shrinkage stresses in a range of 30 MPa occur at the inner wraps.

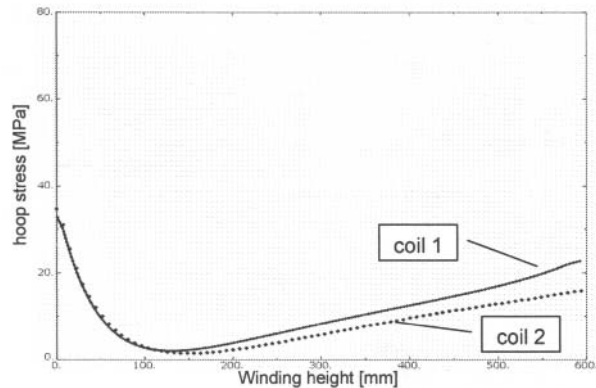


Figure 7: Hoop stress of cross sectional cuts in radial direction after storage (see fig. 3)

The effect of relaxation is similar in the outer wraps in width direction, as illustrated in fig. 8. There are smoothed stress progressions for coil 1 and 2 after storage and the hoop stress is drastically reduced, e.g. the maximum value of coil 1 drops from 80 MPa to ~20 MPa.

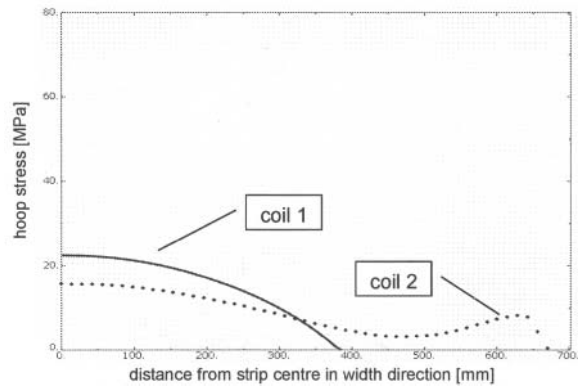


Figure 8: Hoop stress for cross sectional cuts in the outer wrap after storage (see fig. 3)

De-coiling and cutting

Following the coil storage, the resulting flatness of the strips after de-coiling needs to be determined, since this is a decisive quality parameter for the product. During storage, stresses inside the coil are re-distributed due to the transformation of elastic strains into creep strains. This induces local length changes in the strip. Differential lengths of single longitudinal strip fibres cause the formation of residual stresses since the strip must remain a continuous body. By unwinding and cutting of a strip segment, the stresses are partially released and may cause unflatness of a strip resting on a table without further external tensions. The flatness changes of both coils are assessed by considering single wraps of different radial positions of the coils and performing a buckling analysis for a finite section of the wraps. The previously simulated creep strains are interpreted as a differential lengths deviation and used to calculate the local residual stress tensor σ_{res} in the de-coiled strip as follows:

$$\sigma_{res}(x) = -[\varepsilon_{cr}(x) - \bar{\varepsilon}_{cr}] \cdot E_{Al} \quad (2)$$

with the local creep strain ε_{cr} and the Young's modulus of aluminium E_{Al} . The quantity $\bar{\varepsilon}_{cr}$ denotes the average of the creep strain over the strip width.

Fig. 9 visualizes the residual stress in coil 1 after the simulated period of storage calculated according to eqn. (2). The respective residual stress field of a certain wrap of the coil is transferred to a FE-model, mapping a finite section of the wrap, free from external tensions. In particular the FE-analysis considers a finite plate with a dimension of 1400 mm x 2500 mm. Standard shell elements, S4R, are used for discretization. In a first step of the analysis the redistribution of the initial residual stress fields in the released plate is predicted and thereafter buckling of the strip is initiated and simulated. Note that dead loads have been neglected throughout the buckling analysis.

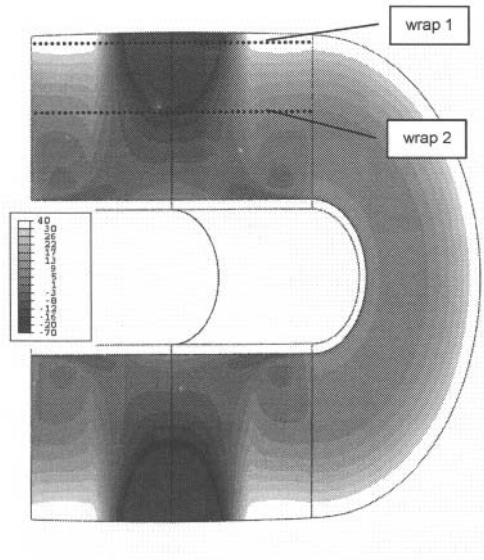


Figure 9: Residual tangential stress in coil 1 before de-coiling after storage

For each coil the buckling analysis is conducted for two wraps, as indicated in fig. 9. The buckling pattern of the final state of coil 1, wrap 1, is presented in fig. 10. A considerable change of the initial flatness can be observed, which originally had been produced at the cold rolling mill. The tendency of long edges is completely removed and a newly developed waviness appears after de-coiling. The buckling pattern of wrap 1 is a superposition of long- and short-wave fractions. The long-wave fraction is a global deflection of the complete plate and acts homogeneously over the strip width. The short-wave fraction of the buckling pattern is localized in the centre of wrap 1 and forms the bags.

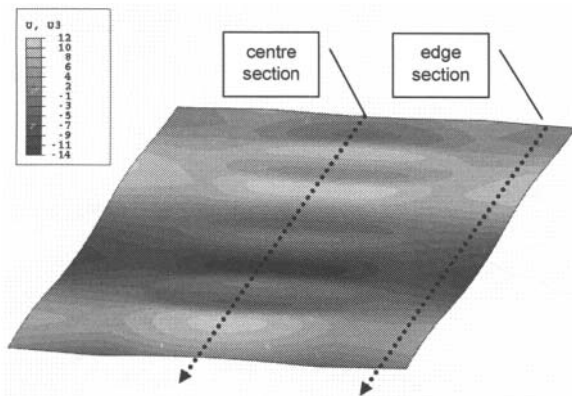


Figure 10: Out-of-plane deformation u_3 [mm] for coil 1, wrap 1 (see fig. 9)

The transition of flatness with respect to the wound height of coil 1 is demonstrated by the out-of-plane deformation u_3 for longitudinal sections as indicated in fig. 10. The results plotted in fig. 11 concentrate on a centre and edge section of wrap 1, whereas fig. 12 presents the respective graphs for wrap 2. The

simulations demonstrate that centre buckles are to be expected most likely on the outer part of coil 1, i.e. in wrap 1.

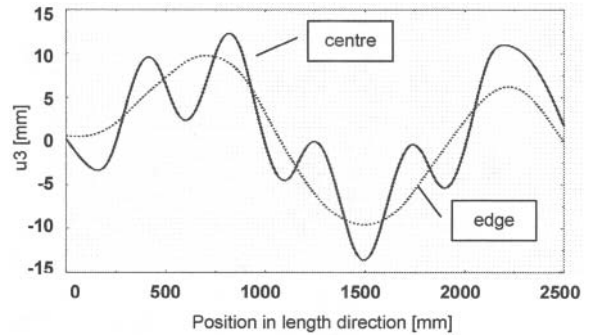


Figure 11: Out-of-plane deformation for longitudinal sections of coil 1, wrap 1, at the centre (straight line) and edge (dotted line)

Wrap 2 is more or less dominated by a homogeneous long-wave deflection, with no tendency of short-wave bag formation.

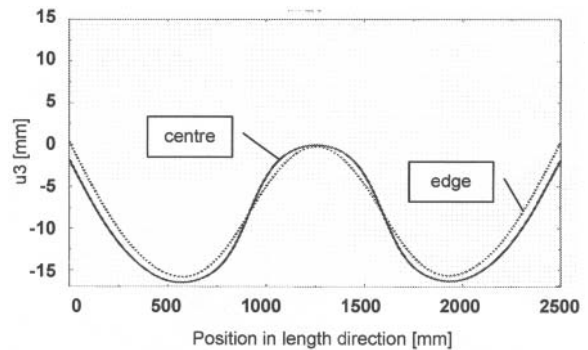


Figure 12: Out-of-plane deformation for longitudinal sections of coil 2, wrap 1, at the centre (straight line) and edge (dotted line)

The buckling analysis of coil 2 is presented in fig. 13 for wrap 1. The simulation reflects the impact of the up-coming edges in the thickness profile. The corresponding formation of a hoop stress peak (see fig. 5) creates bags, resp. waviness, at the edges of wrap 1. As observed for coil 1 the general trend of a positive crown in the profile forms centre buckles in the final flatness of the outer wraps of the coil. But the lower total profile magnitude and the large bearing fraction in the profile of coil 2 creates a better flatness quality of the plate. This is confirmed by the maximum values of out-of-plane deformation u_3 . The amplitude of u_3 of coil 2 amounts to 15 mm in contrast to coil 1 where the corresponding value is in a range of 26 mm.

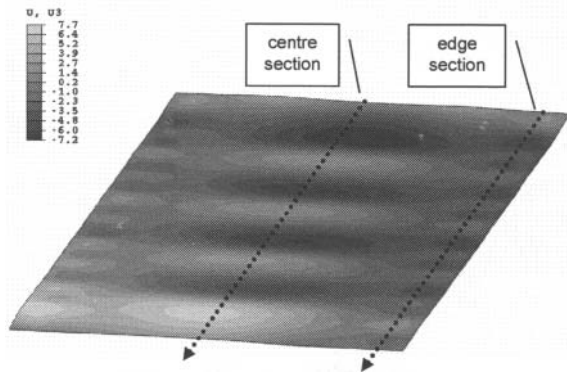


Figure 13: Out-of-plane deformation u_3 [mm] for coil 2, wrap 1 (see fig. 9)

The flatness of coil 2, wrap 1 plotted on longitudinal sections in fig. 14 shows less long-wave fractions. This is most likely the consequence of the lower total profile and the superior bearing fraction resulting in lower residual stresses to be released.

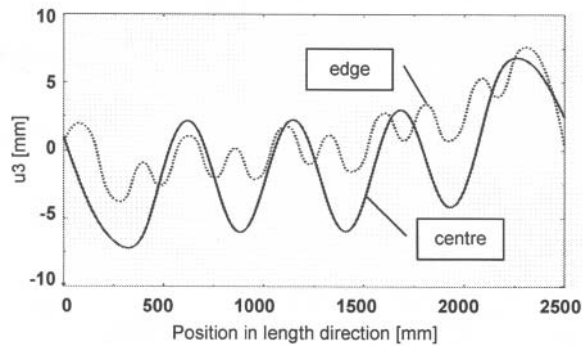


Figure 14: Out-of-plane deformation for longitudinal sections of coil 2, wrap 1, at the centre (straight line) and edge (dotted line)

In fig. 15 the same analysis is plotted for the inner wrap 2. The flatness is dominated by a long-wave deflection of the complete plate. The centre buckles nearly completely disappear. The effect of the upcoming edges seems to persist even at the interior parts of the coil which show low frequency waves.

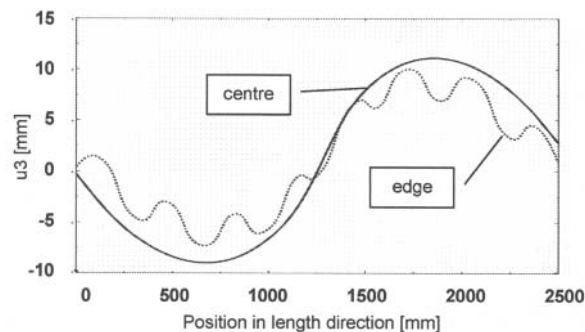


Figure 15: Out-of-plane deformation for longitudinal sections of coil 2, wrap 2, at the centre (straight line) and edge (dotted line)

Conclusion

The application of various models along the processing chain of aluminium strips has been demonstrated with a view of predicting the flatness of the final product. A special focus has been put on the through process character of the flatness development.

It could be shown that the flatness of a 0.28 mm thick sheet is already determined by the strip condition exiting the hot mill at a gauge of 5 mm. It was demonstrated, that the profile in this condition can take effect in the final product by causing inhomogeneous stress distributions inside the wound coil, which can partially relax, depending on alloy, winding parameters and storage conditions. Upon unwinding and cutting, the remaining residual stresses are set free and the plate deforms elastically on a flat table without further external loads. The plate develops characteristic wave patterns in different positions over the width which also vary along the total length upon unwinding.

The use of the through process model allows the detection of flatness relevant mechanisms in the processing chain. Thus it is possible to develop adequate rolling and winding strategies in order to improve final quality or to minimize leveling operations.

References

- [1] K.F.Karhausen, M.Wimmer: Walzen von Flachprodukten, Hrsg. J.Hirsch, Wiley-VCH (2001) p.89-98
- [2] R.B. Cresdee, W.J.Edwards, P.J.Thomas, Iron and Steel Engineer, Vol.68, No.10, 1991, 41-51
- [3] James K. Good, David R. Roissum, *Winding: Machines, Mechanics and Measurements*, Norcross: Tappi Press, 2007.
- [4] M. Wimmer, "Simulation des Wickelns von Bandhalbzeugen aus Aluminium", PhD, thesis RWTH Aachen, 2005.
- [5] M. Wimmer, A. Cremer, S. Neumann, K. Karhausen, "Optimisation the winding of Al- strip", Proc. TMS 2009.
- [6] NN: Abaqus Users Manual, Version 6.10, 2010.